Structural basis for selective inhibition of purine nucleoside phosphorylase from *Schistosoma mansoni*: Kinetic and structural studies

Marcelo S. Castilho [a,*], Matheus P. Postigo [b], Humberto M. Pereira [b], Glaucius Oliva [b], Adriano D. Andricopulo [b,*]

[a] *Universidade Federal da Bahia, Faculdade de Farmácia, R. Barão de Jeremoabo, s/n, 40170-115, Salvador-BA, Brazil*
[b] *Laboratório de Química Medicinal e Computacional, Centro de Biotecnologia Molecular Estrutural, Instituto de Física de São Carlos, Universidade de São Paulo, 13566-970 São Carlos-SP, Brazil*

ARTICLE INFO

ABSTRACT

Selectivity plays a crucial role in the design of enzyme inhibitors as novel antiparasitic agents, particularly in cases where the target enzyme is also present in the human host. Purine nucleoside phosphorylase from *Schistosoma mansoni* (*Sm*PNP) is an attractive target for the discovery of potential antischistosomal agents. In the present work, kinetic studies were carried out in order to determine the inhibitory potency, mode of action and enzyme selectivity of a series of inhibitors of *Sm*PNP. In addition, crystallographic studies provided important structural insights for rational inhibitor design, revealing consistent structural differences in the binding mode of the inhibitors in the active sites of the *Sm*PNP and human PNP (*Hs*PNP) structures. The molecular information gathered in this work should be useful for future medicinal chemistry efforts in the design of new inhibitors of *Sm*PNP having increased affinity and selectivity.

© 2010 Elsevier Ltd. All rights reserved.

1. Introduction

Purine nucleoside phosphorylase (PNP, EC 2.4.2.1) is a key enzyme in the purine salvage pathway which has been primarily studied as a target for the treatment of T-cell proliferative diseases, such as T-cell leukemias or lymphomas, organ transplant rejection, rheumatoid arthritis, psoriasis, and some other autoimmune diseases.[1–3] More recently, it has been suggested that selective inhibitors of PNP could also be used for the therapy of major parasitic infectious diseases, such as malaria and schistosomiasis.[1,4–7]

According to the World Health Organization, schistosomiasis is the second most important tropical parasitic disease, affecting about 200 million people worldwide, with more than 650 million living in endemic areas.[8] Even though praziquantel is an effective drug for the treatment of the disease, it has been in use for more than 20 years and recent reports indicate that significant resistance to the drug may be present in different geographic locations.[9]

The identification and study of novel molecular targets as well as the development of new drugs to treat this and other neglected tropical diseases are of utmost importance in drug discovery.[10–12] The parasite *Schistosoma mansoni*, one of the etiologic agents of human schistosomiasis, lacks the de novo pathway for purine biosyn-

thesis and depends entirely on the salvage pathway for its purine requirements for synthesis of RNA and DNA.[6,13] Taking into account that PNP from *S. mansoni* (*Sm*PNP) is an important component of the purine salvage pathway and has been identified as an attractive drug target, the use of potent and selective inhibitors can cause purine starvation, leading to death of the parasite.[1,4,6]

Structure-based approaches have become vital components in the design of enzyme inhibitors and receptor ligands.[11,14] Previously, we have crystallized *Sm*PNP and determined its three-dimensional structure in complex with different ligands.[6] As part of our ongoing research program aimed at discovering selective inhibitors of the parasite enzyme, we have carried out kinetic and crystallographic studies on a series of deazaguanines and other modified purine bases. The biochemical and structural studies revealed important molecular requirements for PNP binding affinity and selectivity.

2. Experimental

*Sm*PNP was expressed and purified as described previously.[4,6] Human PNP (*Homo sapiens*, *Hs*PNP) from CalBioChem and xanthine oxidase from Sigma Aldrich were the best grades available and used without further purification. The PNP inhibitors **1–8** employed in this work were synthesized by scientists at BioCryst Pharmaceuticals Inc.[15] and are the gift of that organization. The compounds **9** and **10** were purchased from Sigma Aldrich. Other

---

* Corresponding authors. Tel.: +55 16 3373 8095; fax: +55 16 3373 9881 (A.D.A.).
E-mail addresses: castilho@ufba.br (M.S. Castilho), aandrico@ifsc.usp.br (A.D. Andricopulo).

reagents were obtained commercially from Sigma Aldrich and were of the highest purity available.

2.1. Kinetic measurements

Kinetic measurements were carried out spectrophotometrically with the aid of a Cary100 UV–vis spectrophotometer, using a standard coupled assay as previously described.[16,17] The reaction mixture contained 5 nM SmPNP (as the monomer), 50 mM phosphate buffer (KPO_4, pH 7.4), 10 μM inosine, and xanthine oxidase 40 milliunits/mL. Uric acid formation was monitored at 293 nm, in triplicate at 25 °C (extinction coefficient for uric acid, ϵ_{293} = 12.9 mM^{-1}).[18] No inhibition of the coupled enzyme was observed in all experiments. Values of IC_{50} were independently determined by making rate measurements for at least six inhibitor concentrations. The type of inhibition was determined under the same experimental conditions for three different inhibitor concentrations at five varying substrate concentrations (5.0, 7.5, 10.0, 15.0 and 20.0 μM). Kinetic parameters were determined from the collected data employing the SigmaPlot enzyme kinetics module. The values represent means of at least three individual experiments.

2.2. Selectivity assays

To define the selectivity ratio of the inhibitors (human/S. mansoni), the same general experimental protocol described above (item 2.1) was used for the evaluation of the compounds 1–10 against HsPNP. The concentration of inosine was adjusted to 64 μM in order to keep the same [S]/K_M ratio for both enzymes. The selectivity of the inhibitors was expressed in Table 1 as follows:

$$\text{Selectivity} = (IC_{50}^{HsPNP}/IC_{50}^{SmPNP})$$

2.3. Crystallization and soaking of SmPNP

The highly purified SmPNP enzyme was crystallized as described previously.[4,6] Next, crystals grown at 4 °C in 20% PEG 1500, 15 mM sodium acetate buffer (pH 4.9 or 5.0) and 20% glycerol (buffer A) were then soaked for 48–96 h in solutions containing up to 2.5 mM of compounds 4, 8, 9, 10 or guanosine, respectively, dissolved in 1:9 DMSO/buffer A.

2.4. X-ray data collection and structure refinement

X-ray diffraction data were collected at 100 K at MX1 beamline of the LNLS (National Laboratory of Synchrotron Light, in Campinas - Brazil). The crystals of SmPNP in complex with guanosine (SmPNP-GUA) diffracted up to 2.05 Å. The data were indexed and integrated using the program MOSFLM[19] and scaled using the program SCALA from the CCP4 suite.[20] Next, the complex SmPNP-

Table 1
Structures of compounds 1–10 and values of IC_{50} on Schistosoma mansoni PNP and human PNP
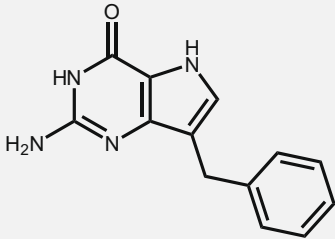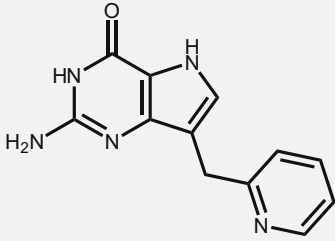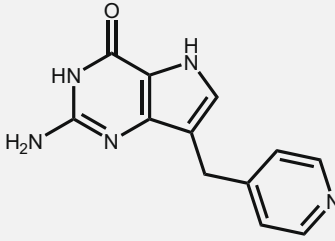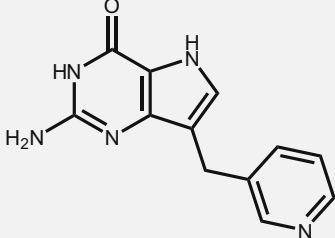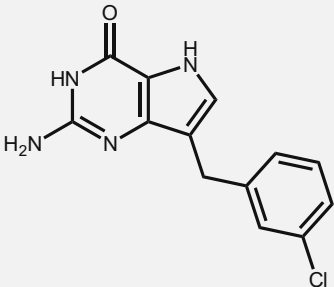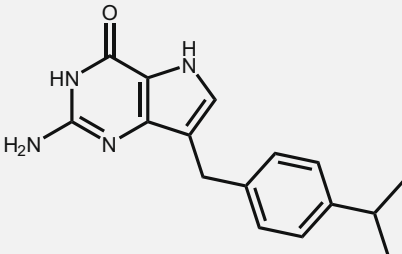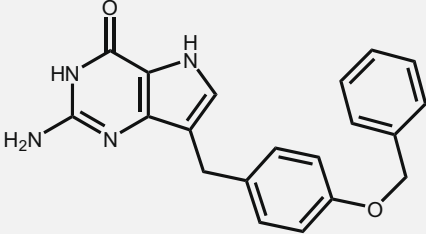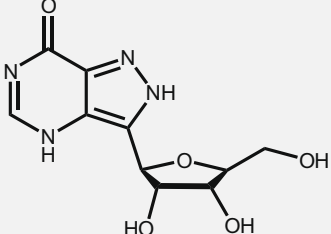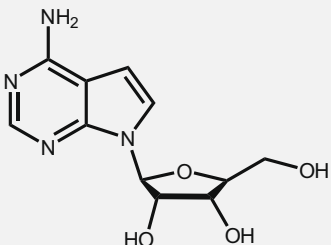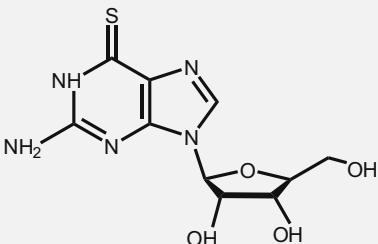
Compd	Structure	IC_{50}^{SmPNP} (μM)[a]	IC_{50}^{HsPNP} (μM)[a]	Selectivity for SmPNP[b]
1		1.4 ± 0.09	0.06 ± 0.003	0.043
2		7.0 ± 0.8	0.023 ± 0.001	0.003
3		3.0 ± 0.4	0.1 ± 0.007	0.033
4		0.8 ± 0.05	0.2 ± 0.008	0.25

Table 1 (continued)

Compd	Structure	IC_{50}^{SmPNP} (µM)[a]	IC_{50}^{HsPNP} (µM)[a]	Selectivity for SmPNP[b]
5		0.5 ± 0.03	0.05 ± 0.003	0.1
6		0.15 ± 0.01	0.27 ± 0.03	1.8
7		0.5 ± 0.08	0.3 ± 0.01	0.6
8		47 ± 3.8	300 ± 19	6.4
9		200 ± 17	300 ± 23	1.5
10		95 ± 6.6	315 ± 27	3.3

[a] The values represent means of three individual experiments ± SD.
[b] Selectivity is given by the ratio $IC_{50}^{HsPNP}/IC_{50}^{SmPNP}$.

GUA was solved by molecular replacement using SmPNP in complex with acetate (PDB ID 1TD1) as the search model, as available in Molrep.[21] The refinement was carried out using Refmac,[22] and the model building was performed with Coot,[23] using σ_a-weighted $2F_o$–F_c and F_o–F_c electron density maps. The compounds were automatically placed using the 'Find Ligand' routine of Coot. Addi-

Table 2
X-ray data collection and refinement parameters for the crystallographic structure of *Sm*PNP in complex with guanosine

Full data collection and refinement statistics	
Space group	$P2_12_12_1$
Cell dimensions (Å)	$a = 48.21$; $b = 118.19$; $c = 129.36$
Detector	MarCCD 165
X-ray source	LNLS MX1
Wavelength (Å)	1.43
Resolution range (Å)	43.6–2.05 (2.16–2.05)*
Redundancy	3.1 (2.6)*
R_{meas} (%)	5.8 (41.4)*
R_{sym} (%)	4.9 (34.1)*
Completeness (%)	94.1 (85.4)*
Total reflections	138,890
Unique reflections	44,386
$I/\sigma I$	13.3 (2.5)*
Refinement parameters	
R (%)	17.5
R_{Free} (%)	23.4
Ramachandran plot	
Most favoured region (%)	91.8
No. residues in disallowed regions	3
Overall B-factor (Å^2)	37.02
Ligand B-factor(Å^2)	40.97
No protein atoms	6237
No water molecules	565
No ligand atoms	62
r.m.s. bond lengths (Å)	0.006
r.m.s. bond angles (Å)	1.04

* Values in the last shell.

tional manual building and placement of water molecules were performed using the Coot software. R and R_{free} parallel reduction were pursued throughout refinement, so that no over fitting occurred. Data collection and processing parameters are collected in Table 2. The coordinates and structures factors of *Sm*PNP-GUA complex are deposited in the PDB under ID 3IEX.

3. Results and discussion

The development of new antiparasitic agents is one of the most important challenges of the 21st century. The limited existing drugs have many side effects or they lose their effectiveness over time. A remarkable difficulty in the study of new antiparasitic compounds lies in the high level of amino acid sequence identity between target enzymes of parasites and their mammalian hosts. A promising approach to tackle this problem is structure-based drug design (SBDD).[24,25] The understanding and comparison of kinetic and structural data of target enzymes in the parasite and its human host, and the subsequent use of the combined information so as to develop molecules that bind selectively to the parasite enzyme is an important rationale behind the design of chemotherapeutic agents.

Although several purine derivatives and other related compounds have been described in the literature as inhibitors of both human and bovine PNPs (*Hs*PNP; and *Bos Taurus*, *Bt*PNP, respectively),[1,3,26–32] no structure–activity relationship (SAR) studies have been conducted to date to investigate inhibitors of *Sm*PNP. Interestingly, *Hs*PNP and *Bt*PNP share approximately 50% identity to *Sm*PNP (Fig. 1), and it is reasonable to assume that selective inhibition of the parasite enzyme is a particularly attractive approach for drug design. However, this is not a simple task as the differences in the active site of *Sm*PNP are limited to the residues Tyr202 and Ser247 (Phe200 and Val245 are the corresponding residues in *Hs*PNP).[4,6,8] In order to better understand and explore the molecular aspects involved in enzyme selectivity, we have determined values of concentrations required for 50% inhibition (IC$_{50}$) of both *Sm*PNP and *Hs*PNP for a series of 9-substituted-9-deazaguanines and other purine analogs, as shown in Table 1. Due to the differences in the K_M values (K_M^{HsPNP} = 41 μM; and K_M^{SmPNP} = 6.4 μM) of the enzymes, we used the same [S]/K_M ratio of 1.56 in all experiments in order to assure quantitative comparisons of binding affinity and selectivity.

The compounds **1–10** showed significant inhibition with IC$_{50}$ values varying in the range of 0.15–200 μM and 0.023–315 μM for the *Sm*PNP and *Hs*PNP enzymes, respectively. Although the parasite and human enzymes were sensitive to these inhibitors, as reflected by the IC$_{50}$ values of Table 1, it can be seen that the 9-substituted-9-deazaguanines (**1–7**) exhibited pronounced selectivity towards the human enzyme (from about 2 to 300-fold). The only exception was inhibitor **6**, which was slightly selective for the parasite enzyme (1.8-fold). In general, the exploration of SARs in drug design is mostly focused on activity against single targets, as it has been the case in the long history of the development of PNP inhibitors. Because many compounds have the potential to
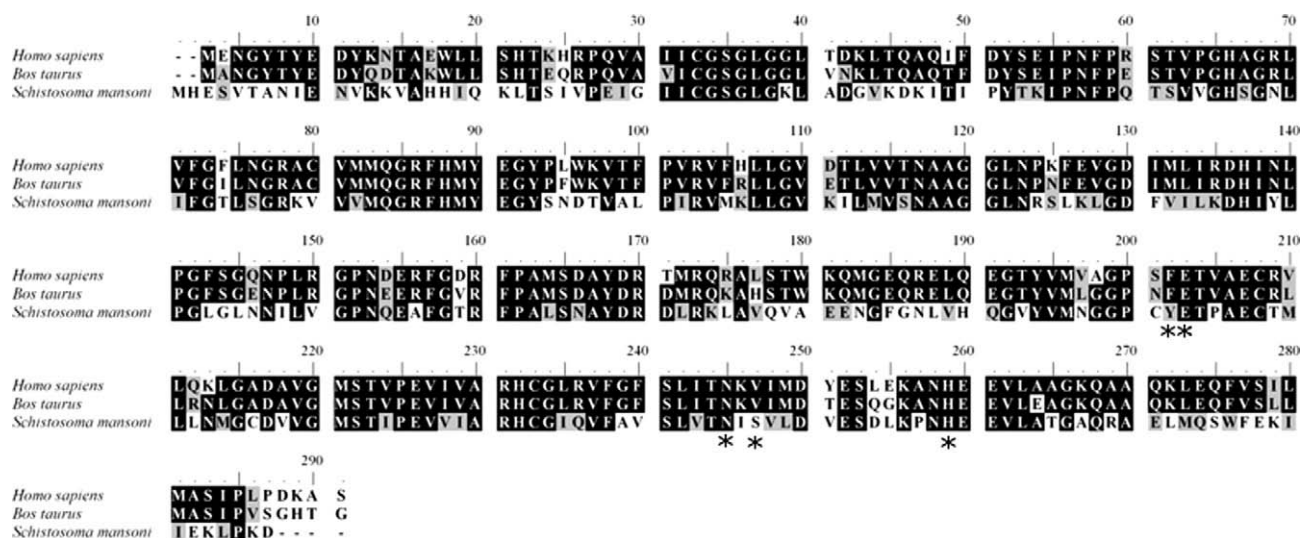

Figure 1. Sequence alignment of bovine (1st lane), human (2nd lane) and *Schistosoma mansoni* (3rd lane) PNPs. Pairwise alignment with BLOSUM62 matrix shows that *Hs*PNP:*Bt*PNP and *Hs*PNP:*Sm*PNP share 86% and 47% identical residues, respectively. Conserved residues are highlighted in gray and identical residues in black. Residues that participate in the catalytic mechanism and influence ligand binding are marked with asterisks (*). The alignment was carried out with the CLUSTALW program.
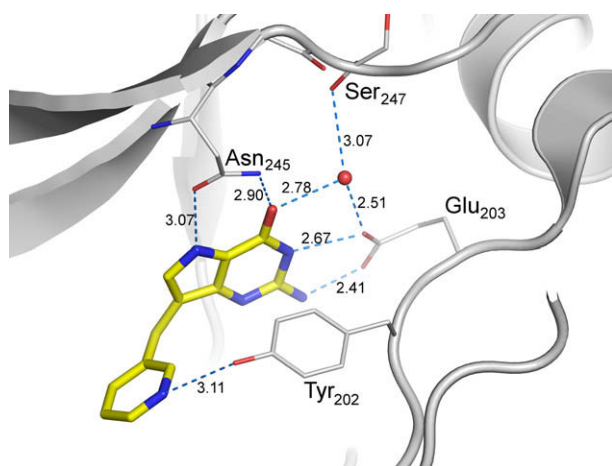
Figure 2. H-bonding network of compound **4** in the active site of *Sm*PNP (PDB ID 3DJF). Residues, as well as a conserved water molecule that interact to **4** are highlighted in the protein structure. Oxygen atoms are depicted in red, nitrogen atoms in blue and carbon atoms are represented in gray (protein) or yellow (**4**). The same color scheme was used in all figures.

act against similar targets (e.g., homologous proteins), achieving a sufficient degree of target selectivity is a major issue for lead optimization. Therefore, in the present work we have analyzed the selectivity data in order to identify useful SARs and structure–selectivity relationships (SSRs) within this series. Particularly, the deazaguanine analogs (**1–7**) are PNP inhibitors exhibiting IC_{50} values in the range from 0.15 to 7.0 μM and from 0.023 to 0.3 μM, respectively, for *Sm*PNP and *Hs*PNP. The selectivity observed in this case is not surprising, since deazaguanines are well-known inhibitors of the mammalian PNPs.[1,3,26–33] On the other hand, the nucleoside analogs (**8–10**) showed good selectivity towards the parasite enzyme (from about 2 to 6.4-fold).

This set of compounds with different activity against the two PNPs, allowed SSRs to be quantitatively described and categorized. Our results suggest that the electronic, H-bonding, volume and hydrophobicity properties correlate with the inhibitory potency of these compounds. As noted in Table 1, the *ortho*- (**2**) and *para*-(**3**) pyridine-substituted derivatives afforded an improvement in selectivity towards the *Hs*PNP compared to the parent compound **1** (14 and 1.3-fold, respectively), whereas the corresponding *meta*-substituted pyridine (**4**) showed a moderate shift towards the opposite way, being sixfold less selective than compound **1** for the human enzyme. X-ray structural data is very useful to reveal three-dimensional (3D) molecular interactions involved in enzyme inhibitor complexes.[34,35] A careful analysis of the crystallographic complex between the inhibitor **4** and *Sm*PNP (PDB ID 3DJF) indicates that this might be a result of the H-bonding to Tyr202 (Fig. 2).

For that reason, the *meta*-Cl substituted analog (**5**) was investigated, and, unexpectedly, the selectivity towards *Sm*PNP slightly decreased. On the other hand, compound **6** having an isopropyl group at the *para*-position of the phenyl ring exhibited not only improved potency ($IC_{50}^{SmPNP} = 0.15$ μM), but also selectivity towards *Sm*PNP, with an interesting selectivity ratio of 1.8. However, the presence of a bulkier group at the *para*-position of the phenyl ring (compound **7**) showed that a loss in selectivity was accompanied by a decreasing in potency. This fact may be a consequence of the increased molecular volume and lipophilicity, which is associated with reduced target selectivity.[36] For that reason, we focused on inhibitors bearing a slightly hydrophilic ribose moiety at the 9-position of the base ring. Although the compounds **8–10** exhibited a relatively modest inhibitory potency, their selectivity rates are considerably superior to those observed for compounds **1–6**. Par-
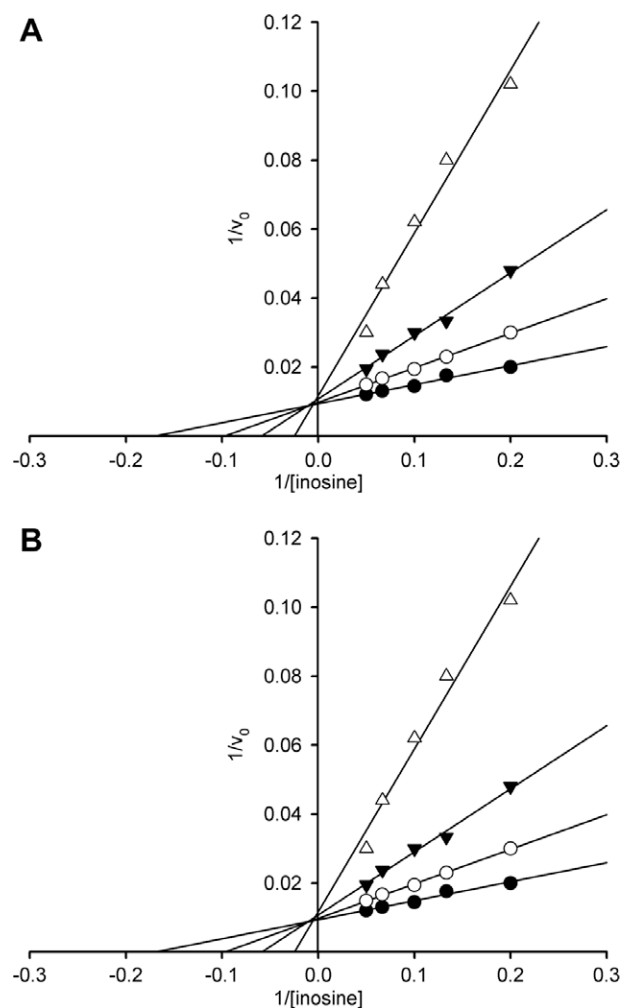

Figure 3. Competitive inhibition profile of compounds **4** (A) and **6** (B) against *Sm*PNP. Kinetic experiments were conducted in the presence of increasing concentrations of the inhibitors. Panel A: 0.8 μM (○), 1.6 μM (▼) and 3.0 μM (△). Panel B: 150 nM (○), 300 nM (▼) and 600 nM (△). The absence of inhibitor is depicted by ● in panels A and B.

ticularly, compound **8** is the most potent of the series **8–10** and possess over sixfold selectivity towards the parasite enzyme. These are very important molecular aspects, which need to be understood. Because the mode of inhibitor type defines the binding relationships between the free enzyme (E), substrate (S) and enzyme–substrate (E·S) species to the inhibitor (I), we have determined the type of inhibition of this series of compounds with respect to the physiological substrate for *Sm*PNP, in order to allow the development of mechanism-based SSRs (Fig. 3).

The results of the Lineweaver–Burk double-reciprocal plots shown in Figure 3 indicate that the inhibition of *Sm*PNP was found to be competitive with respect to inosine (compounds **4** and **6** were chosen as representative members of this series of inhibitors). The same mode of inhibitor action had previously been observed for the human and bovine PNPs, in which the inhibitors exclusively binds to the free enzyme, in direct competition with the substrate.[16,17] As one would expected, the presence of a competitive inhibitor affects the formation of the (E·S) complex (apparent value of K_M) but not the subsequent chemical steps following the E·S formation (V_{MAX}).[37] The double-reciprocal plots of the velocity as a function of substrate at varying concentrations of the inhibitors **4** and **6** (Fig. 3) show that the values of V_{MAX} remained unchanged at all inhibitor concentrations (set of lines that intercept the y-axis, $1/V_{MAX}$), whereas the apparent values of

K_M (the *x*-intercept lines, $-1/K_M$) increased with increasing inhibitor concentration by a factor of $(1 + [I]/K_i)$. The same behavior was observed for the other inhibitors presented in Table 1 (results not shown).

Considering that the studied inhibitors present a pure competitive mechanism with all trimeric PNPs, it is appropriate to analyze the molecular aspects involved in the interactions of these compounds within a common active site on the enzymes. In this work, we have extended our crystallographic studies to further investigate the binding mode of this series of selective inhibitors into the substrate binding cavity of *Sm*PNP. A series of soaking and X-ray data collection experiments were carried out to determine the crystallographic structure of *Sm*PNP in complex with compounds **8–10**. While no success was achieved after several attempts, we obtained a novel crystallographic structure of *Sm*PNP in complex with guanosine (PDB ID 3IEX) at 2.05 Å (Table 2 and Fig. 4). This complex is particularly interesting due to the high similarity between the structures of guanosine and inhibitor **8**. In addition, we compared the obtained crystallographic structure with that of *Hs*PNP in complex with guanosine (PDB ID 1RFG) in order to provide useful insights into the molecular aspects involved in the *Sm*PNP selectivity exhibited by inhibitors **8–10**.

Interestingly, a detailed comparison of the molecular interaction profile of guanosine into the active sites of *Sm*PNP and *Hs*PNP (Fig. 5) revealed that a more extensive H-bonding network is present in the purine binding site of the parasite enzyme, in which a crystallographic water molecule is held into place by the residues Glu203 and Ser247 (Glu201 and Val245 are located in the equivalent positions of the human enzyme). This structural evidence highlights the importance of the Ser247 side chain in the *Sm*PNP-GUA complex. Furthermore, the O5' of the ribose ring forms a hydrogen bond to Tyr202, assisting the binding of guanosine to the *Sm*PNP active site. Importantly, as can be seen in Figure 5, a similar intermolecular interaction is prevented in the human and bovine counterparts as they have a Phe200 residue in the corresponding position.

The understanding of the structural and chemical basis for molecular recognition, binding mode, reaction mechanism and biological activity remains a major challenge in drug design. The kinetic results showed that the inhibitors in the present study act competitively in the presence of the physiological substrate for both parasite and human PNP enzymes. The structural data indicate that the purine-ribose derivatives form a hydrogen bond with Tyr202, which may play an important role in the design of *Sm*PNP-selective inhibitors. The integration of kinetic and crystal-
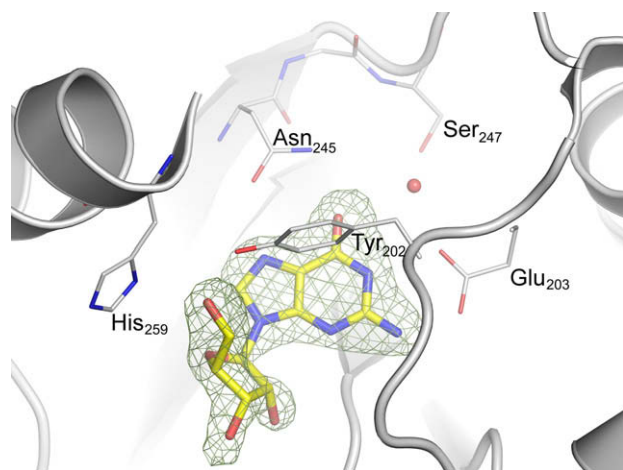

Figure 5. Interaction profile of guanosine in the active site of *Sm*PNP (A) and *Hs*PNP (B). The dashed lines indicate that the residue Tyr202 participates in the binding of guanosine to *Sm*PNP, (not possible in the case of *Hs*PNP).

lographic studies and the subsequent development of preliminary SARs and SSRs were useful tools not only for the identification of molecular requirements for binding affinity, but also for the understanding of the structural basis for enzyme selectivity within this series of PNP inhibitors.

References notes

1. Bzowska, A.; Kulikowska, E.; Shugar, D. *Pharmacol. Ther.* **2000**, *88*, 349.
2. Kelley, J. L.; McLean, E. W.; Crouch, R. C.; Averett, D. R.; Tuttle, J. V. *J. Med. Chem.* **1995**, *38*, 1005.
3. Montgomery, J. A. *Med. Chem. Rev.* **1993**, *13*, 209.
4. Pereira, H. M.; Cleasby, A.; Pena, S. D.; Franco, G. R.; Garratt, R. C. *Acta Crystallogr., Sect. D* **2003**, *59*, 1096.
5. Kicska, G. A.; Tyler, P. C.; Evans, G. B.; Furneaux, R. H.; Schramm, V. L.; Kim, K. *J. Mol. Biol.* **2002**, *277*, 3226.
6. Pereira, H. D.; Franco, G. R.; Cleasby, A.; Garratt, R. C. *J. Mol. Biol.* **2005**, *353*, 584.
7. Shi, W.; Ting, L. M.; Kicska, G. A.; Lewandowicz, A.; Tyler, P. C.; Evans, G. B.; Furneaux, R. H.; Kim, K.; Almo, S. C.; Schramm, V. L. *J. Biol. Chem.* **2004**, *279*, 18103.
8. http://www.who.int/mediacentre/factsheets/fs115/en/. Accessed in June 2009.
9. Sabra, A. N.; Botros, S. S. *J. Parasitol.* **2008**, *94*, 537.

Figure 4. Crystallographic structure of guanosine in complex with *Sm*PNP (PDB ID 3IEX). An electron omit map, contoured at 4.0 σ, clearly shows that guanosine is bound to the active site of the enzyme.
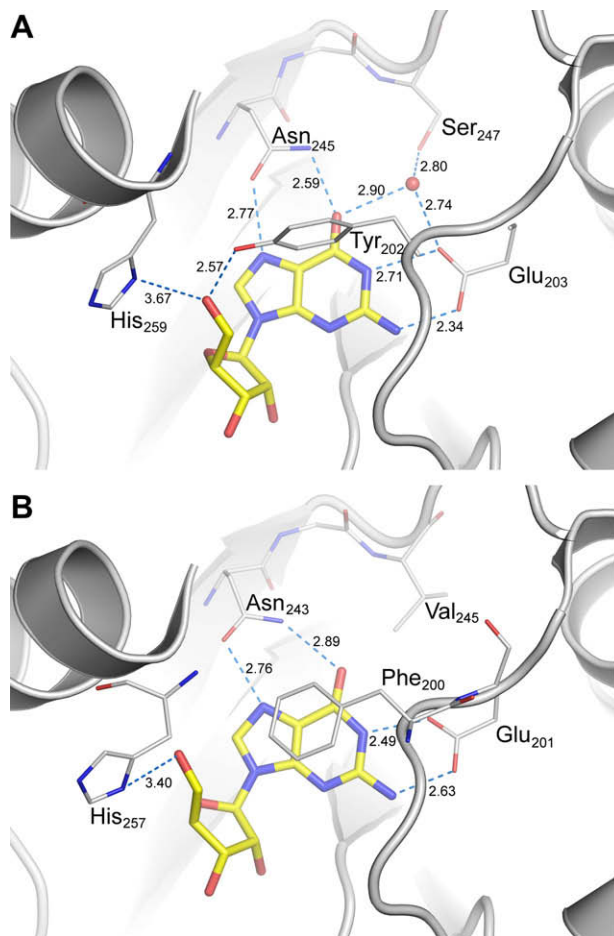
10. Andricopulo, A. D.; Montanari, C. A. *Mini-Rev. Med. Chem.* **2005**, *5*, 585.
11. Guido, R. V. C.; Oliva, G.; Andricopulo, A. D. *Curr. Med. Chem.* **2008**, *15*, 37.
12. (a) Andricopulo, A. D.; Willain, A.; Correa, R.; Correa, A. R. S.; Nunes, R. J.; Yunes, R. A.; Cechinel, V. *Pharmazie* **1998**, *53*, 493; (b) Andricopulo, A. D.; Akoachere, M. B.; Krogh, R.; Nickel, C.; McLeish, M. J.; Kenyon, G. L.; Arscott, L. D.; Williams, C. H.; Davioud-Charvet, E.; Becker, K. *Bioorg. Med. Chem. Lett.* **2006**, *16*, 2283.
13. Senft, A. W.; Crabtree, G. W. *Biochem. Pharmacol.* **1977**, *26*, 1847.
14. Pereira, H. D.; Berdini, V.; Cleasby, A.; Garratt, R. C. *FEBS Lett.* **2007**, *581*, 5082.
15. (a) Elliott, A. J.; Morris, P. E.; Petty, S. L.; Williams, C. H. J. *Org. Chem.* **1997**, *62*, 8071; (b) Elliott, A. J.; Walsh, D. A.; Morris, P. E. US Pat. Appl. Publ., 2,004,254,181, 2004.; (c) Secrist, J. A.; Montgomery, J. A.; Ealick, S. E.; Erion, M. D.; Guida, W. C. US Pat 4,985,433, 1991.; (d) Pathak, V. P. *Org. Process Res. Dev.* **2000**, *4*, 129; (e) Montgomery, J. A.; Niwas, S.; Rose, J. D.; Secrist, J. A.; Babu, Y. S.; Bugg, C. E.; Erion, M. D.; Guida, W. C.; Ealick, S. E. *J. Med. Chem.* **1993**, *36*, 55; (f) Acton, E. M.; Ryan, K. J.; Henry, D. W.; Goodman, L. J. *Chem. Soc., D: Chem. Commun.* **1971**, *16*, 986.
16. Farutin, V.; Masterson, L.; Andricopulo, A. D.; Cheng, J.; Riley, B.; Hakimi, R.; Frazer, J. W.; Cordes, E. H. *J. Med. Chem.* **1999**, *42*, 2422.
17. Andricopulo, A. D.; Yunes, R. A. *Chem. Pharm. Bull.* **2001**, *49*, 10.
18. Kim, B. K.; Cha, S.; Parks, R. E., Jr. *J. Biol. Chem.* **1968**, *243*, 1771.
19. Leslie, A. G. W. *Acta Crystallogr., Sect. D* **1999**, *55*, 1696.
20. The CCP4 suite: programs for protein crystallography. *Acta Crystallogr., Sect. D* **1994**, *50*, 760.
21. Vagin, A.; Teplyakov, A. *Acta Crystallogr.* **2000**, *56*, 1622.
22. Murshudov, G. N.; Vagin, A.; Dodson, E. J. *Acta Crystallogr.* **1997**, *53*, 240.
23. Emsley, P.; Cowtan, K. *Acta Crystallogr., Sect. D* **2004**, *60*, 2126.
24. Larson, E. T.; Deng, W.; Krumm, B. E.; Napuli, A.; Mueller, N.; Van Voorhis, W. C.; Buckner, F. S.; Fan, E.; Lauricella, A.; DeTitta, G.; Luft, J.; Zucker, F.; Hol1, W. G. J.; Verlinde, C. L. M. J.; Merritt, E. A. *J. Mol. Biol.* **2008**, *381*, 975.
25. Andricopulo, A. D.; Salum, L. B.; Abraham, D. J. *Curr. Top. Med. Chem.* **2009**, *9*, 771.
26. Castilho, M. S.; Postigo, M. P.; Paula, C. B. V.; Montanari, C. A.; Oliva, G.; Andricopulo, A. D. *Bioorg. Med. Chem.* **2006**, *14*, 516.
27. Erion, M. D.; Niwas, S.; Rose, J. D.; Ananthan, S.; Allen, M.; Secrist, J. A.; Babu, Y. S.; Bugg, C. E.; Guida, W. C.; Ealick, S. E.; Montgomery, J. A. *J. Med. Chem.* **1993**, *36*, 3771.
28. Merino, P.; Tejero, T.; Delso, I. *Curr. Med. Chem.* **2008**, *15*, 954.
29. Clinch, K.; Evans, G. B.; Fröhlich, R. F.; Furneaux, R. H.; Kelly, P. M.; Legentil, L.; Murkin, A. S.; Li, L.; Schramm, V. L.; Tyler, P. C.; Woolhouse, A. D. *J. Med. Chem.* **2009**, *52*, 1126.
30. Kamath, V. P.; Xue, J.; Juarez-Brambila, J. J.; Morris, C. B.; Ganorkar, R.; Morris, P. E., Jr. *Bioorg. Med. Chem Lett.* **2009**, *19*, 2624.
31. Kamath, V. P.; Xue, J.; Juarez-Brambila, J. J. *Bioorg. Med. Chem Lett.* **2009**, *19*, 2627.
32. Secrist, J. A.; Niwas, S.; Rose, J. D.; Babu, Y. S.; Bugg, C. E.; Erion, M. D.; Guida, W. C.; Ealick, S. E.; Montgomery, J. A. *J. Med. Chem.* **1993**, *36*, 1847.
33. Woo, P. W.; Kostlan, C. R.; Sircar, J. C.; Dong, M. K.; Gilbertsen, R. B. *J. Med. Chem.* **1992**, *35*, 1451.
34. Ladame, S.; Castilho, M. S.; Silva, C. H. T. P.; Denier, C.; Hannaert, V.; Perie, J.; Oliva, G.; Willson, M. *Eur. J. Biochem.* **2003**, *270*, 4574.
35. Guido, R. V. C.; Oliva, G.; Montanari, C. A.; Andricopulo, A. D. *J. Chem. Inf. Model.* **2008**, *48*, 918; Honorio, K. M.; Garratt, R. C.; Polikarpov, I.; Andricopulo, A. D. *J. Mol. Graphics Modell.* **2007**, *25*, 921; Salum, L. B.; Polikarpov, I.; Andricopulo, A. D. *J. Chem. Inf. Model.* **2008**, *48*, 2243.
36. Leeson, P. D.; Springthorpe, B. *Nat. Rev. Drug Disc.* **2007**, *6*, 881.
37. Copeland, R. A.. In *Evaluation of Enzyme inhibitors in Drug Discovery: A Guide for Medicinal Chemists and Pharmacologists*; Wiley-Interscience: New Jersey, 2005; Vol. 48.